Gianulis et al., http://www.jgp.org/cgi/content/full/jgp.201310995/DC1

Table S1

Boltzmann fit values for the steady-state activation (G-V) relationships of WT hERG and each hERG [S4–S5]Ala$_{ind}$ mutant channel

Constructs	$V_{1/2}$	k	n
WT	−0.8 ± 2.1	9.0 ± 0.5	7
Δeag	3.2 ± 1.3	11.5 ± 0.9	6
Δeag + N-eag-CFP	−6.7 ± 1.5	9.5 ± 0.7	8
L539A	−3.0 ± 2.4	10.4 ± 0.9	6
Δeag L539A	−0.3 ± 1.5	10.4 ± 0.6	3
Δeag L539A + N-eag-CFP	−6.8 ± 4.5	10.3 ± 1.3	7
D540A	−37.0 ± 6.2[a]	28.4 ± 3.4[a]	6
Δeag D540A	−55.4 ± 2.7[a]	17.0 ± 2.4[a]	6
Δeag D540A + N-eag-CFP	−51.6 ± 4.2[a]	20.7 ± 3.4[a]	7
R541A	−12.5 ± 2.2[b]	6.7 ± 0.3	6
Δeag R541A	−1.4 ± 3.0	9.9 ± 1.5	4
Δeag R541A + N-eag-CFP	−0.9 ± 3.1	10.6 ± 0.5	7
Y542A	−4.6 ± 2.1	7.6 ± 0.8	5
Δeag Y542A	−5.3 ± 2.2	10.4 ± 0.8	6
Δeag Y542A + N-eag-CFP	−1.5 ± 1.5	12.3 ± 0.9	5
S543A	−20.8 ± 3.6[a]	10.6 ± 0.9	5
Δeag S543A	−23.0 ± 3.6[a]	12.7 ± 0.7	4
Δeag S543A + N-eag-CFP	−27.7 ± 0.9[a]	12.4 ± 2.1	5
E544A	1.8 ± 1.8	9.7 ± 0.3	8
Δeag E544A	5.0 ± 3.9	11.1 ± 0.6	5
Δeag E544A + N-eag-CFP	−2.5 ± 5.6	8.8 ± 1.4	5
Y545A	−13.7 ± 2.2[b]	9.8 ± 0.5	6
Δeag Y545A	−6.0 ± 1.4	11.6 ± 1.7	6
Δeag Y545A + N-eag-CFP	−10.5 ± 1.4	8.4 ± 0.5	6

Steady-state activation (G-V) relationships of WT hERG and each hERG [S4–S5]Ala$_{ind}$ mutant channel were fit with a Boltzmann function to yield the $V_{1/2}$ and slope factor (k) values. Data are presented as mean ± SEM. n represents the number of cells.

[a]$P < 0.01$ versus WT hERG (ANOVA).

[b]$P < 0.05$ versus WT hERG.

Table S2

Time constants of deactivation of WT hERG and hERG [S4–S5]Ala$_{ind}$ mutant channels alone and with N-eag-CFP coexpression

Constructs	Tau_f (ms)					Tau_s (ms)					*n*
	Voltage (mV)					Voltage (mV)					
	−120	−100	−80	−60	−40	−120	−100	−80	−60	−40	
WT	23 ± 2	35 ± 2	N/A	254 ± 45	330 ± 53	137 ± 11	176 ± 20	N/A	1,098 ± 124	2,346 ± 284	7
Δeag	9 ± 1	13 ± 3	N/A	33 ± 9	51 ± 7	52 ± 4	65 ± 9	N/A	257 ± 55	391 ± 54	7
Δeag + N-eag-CFP	21 ± 3[a]	32 ± 4[a]	N/A	181 ± 27[a]	234 ± 27[a]	115 ± 18[a]	160 ± 27[a]	N/A	644 ± 83[a]	1,273 ± 175[a]	7
L539A	15 ± 2	18 ± 2	N/A	124 ± 24	229 ± 13	108 ± 12	124 ± 29	N/A	670 ± 106	1145 ± 30	3
ΔeagL539A	6 ± 1	7 ± 1	N/A	17 ± 3	28 ± 2	61 ± 5	73 ± 6	N/A	179 ± 35	344 ± 15	3
ΔeagL539A + N-eag-CFP	11 ± 1[b]	16 ± 2[b]	N/A	66 ± 14[b]	155 ± 41	95 ± 12	133 ± 10[a]	N/A	288 ± 24[b]	739 ± 125	7
D540A	18 ± 1	22 ± 2	N/A	N/A	N/A	141 ± 25	166 ± 16	N/A	N/A	N/A	6
ΔeagD540A	7 ± 2	10 ± 1	N/A	N/A	N/A	32 ± 9	57 ± 10	N/A	N/A	N/A	6
ΔeagD540A + N-eag-CFP	15 ± 3[b]	19 ± 2[a]	N/A	N/A	N/A	68 ± 8[b]	104 ± 11[a]	N/A	N/A	N/A	8
R541A	20 ± 2	26 ± 5	N/A	156 ± 14	240 ± 12	82 ± 8	102 ± 14	N/A	551 ± 37	1,287 ± 49	7
ΔeagR541A	6 ± 1	9 ± 1	N/A	16 ± 2	27 ± 4	28 ± 2	36 ± 6	N/A	124 ± 33	259 ± 65	6
ΔeagR541A + N-eag-CFP	14 ± 2[b]	22 ± 3[a]	N/A	72 ± 19[b]	128 ± 25[a]	64 ± 12[b]	109 13[a]	N/A	224 ± 49	599 ± 101[b]	7
Y542A	11 ± 1	15 ± 2	N/A	46 ± 6	70 ± 5	70 ± 10	88 ± 11	N/A	386 ± 41	706 ± 58	6
ΔeagY542A	7 ± 1	12 ± 1	N/A	28 ± 6	43 ± 3	49 ± 16	85 ± 24	N/A	229 ± 62	502 ± 77	6
ΔeagY542A + N-eag-CFP	6 ± 1	9 ± 1	N/A	21 ± 3	42 ± 2	41 ± 4	71 ± 10	N/A	155 ± 40	509 ± 86	4
S543A	57 ± 6	103 ± 12	N/A	429 ± 46	596 ± 79	393 ± 33	550 ± 36	N/A	2,660 ± 159	4,255 ± 599	8
ΔeagS543A	13 ± 2	16 ± 3	N/A	44 ± 9	43 ± 6	61 ± 8	92 ± 8	N/A	546 ± 6	640 ± 56	4
ΔeagS543A + N-eag-CFP	74 ± 7[a]	126 ± 17[a]	N/A	740 ± 69[a]	358 ± 91[b]	330 ± 48[a]	462 ± 58[a]	N/A	2,400 ± 410[a]	1,916 ± 305[b]	7
E544A	11 ± 1	18 ± 2	N/A	91 ± 11	140 ± 5	49 ± 2	88 ± 5	N/A	458 ± 52	908 ± 80	3
ΔeagE544A	7 ± 1	11 ± 1	N/A	32 ± 8	42 ± 6	32 ± 5	59 ± 7	N/A	348 ± 24	575 ± 54	6
ΔeagE544A + N-eag-CFP	8 ± 2	11 ± 2	N/A	63 ± 19	118 ± 38	38 ± 5	59 ± 9	N/A	344 ± 52	723 ± 138	5
Y545A	12 ± 1	17 ± 1	N/A	77 ± 9	116 ± 10	63 ± 5	76 ± 9	N/A	405 ± 34	888 ± 34	7
ΔeagY545A	3 ± 1	5 ± 1	N/A	8 ± 1	19 ± 2	28 ± 2	46 ± 4	N/A	242 ± 35	500 ± 55	6
ΔeagY545A + N-eag-CFP	11 ± 2[a]	18 ± 3[a]	N/A	82 ± 21[a]	119 ± 23[a]	60 ± 8[a]	91 ± 12[a]	N/A	378 ± 74	615 ± 65	7

Tails produced by stepping to voltages ranging from −120 to −40 mV in 20-mV increments were fit with a double-exponential function to yield the τ_{fast} and τ_{slow} time constants of deactivation. Values are mean ± SEM. N/A, not applicable.

[a]$P < 0.01$ versus hERG Δeag[S4–S5]Ala$_{ind}$ channel alone (ANOVA).

[b]$P < 0.05$ versus hERG Δeag[S4–S5]Ala$_{ind}$ channel alone (ANOVA).

Table S3

Summary of relative FRET efficiency measurements and Fc/Fy calculations

Constructs	RA-RA_0	Fc/Fy	*n*
HERG-Cit. + HERG-CFP	0.16 ± 0.02[a]	1.1 ± 0.2	9
rCB1-YFP + N-eag-CFP	0.01 ± 0.01	1.5 ± 0.1	11
Δeag-Citrine + N-eag-CFP	0.17 ± 0.02[a]	1.7 ± 0.2	11
Δeag L539A-Citrine + N-eag-CFP	0.15 ± 0.03[a]	1.1 ± 0.1	9
Δeag D540A-Citrine + N-eag-CFP	0.18 ± 0.03[a]	1.0 ± 0.1	7
Δeag R541A-Citrine + N-eag-CFP	0.14 ± 0.02[a]	1.2 ± 0.1	12
Δeag Y542A-Citrine + N-eag-CFP	0.15 ± 0.02[a]	1.1 ± 0.1	11
Δeag S543A-Citrine + N-eag-CFP	0.17 ± 0.02[a]	1.1 ± 0.1	11
Δeag E544A-Citrine + N-eag-CFP	0.19 ± 0.04[a]	1.3 ± 0.2	9
Δeag Y545A-Citrine + N-eag-CFP	0.13 ± 0.03[b]	1.4 ± 0.2	9
Δeag [S4-S5]$Ala_{complete}$-Citrine + N-eag-CFP	0.14 ± 0.02[a]	1.1 ± 0.1	10
N-eag-CFP + Δeag ΔCNBHD-Citrine	0.00 ± 0.02	1.1 ± 0.1	11
N-eag-CFP + YFP-CaM_{1234}	0.00 ± 0.01	1.0 ± 0.1	10
N-eag-CFP + C-linker/CNBHD-Citrine	0.12 ± 0.02[a]	1.1 ± 0.1	9
N-eag-CFP + C-linker/CNBHD-YFP	0.16 ± 0.02[a]	1.3 ± 0.1	6
N-eag-Citrine + C-linker/CNBHD-CFP	0.17 ± 0.03[a]	1.1 ± 0.1	7
Δeag-CFP + ΔpCT-Citrine	0.14 ± 0.01[a]	0.9 ± 0.1	9

The relative FRET efficiency (Ratio A–Ratio A_0) and ratio of donor to acceptor fluorescence (Fc/Fy) values are given as mean ± SEM (see Materials and methods). *n* represents the number of cells.

[a]$P < 0.01$ versus rCB1-YFP + N-eag-CFP or N-eag-CFP + YFP-CaM_{1234} (for FRET two-hybrid assay) (ANOVA).

[b]$P < 0.05$ versus rCB1-YFP + N-eag-CFP or N-eag-CFP + YFP-CaM_{1234} (for FRET two-hybrid assay) (ANOVA).

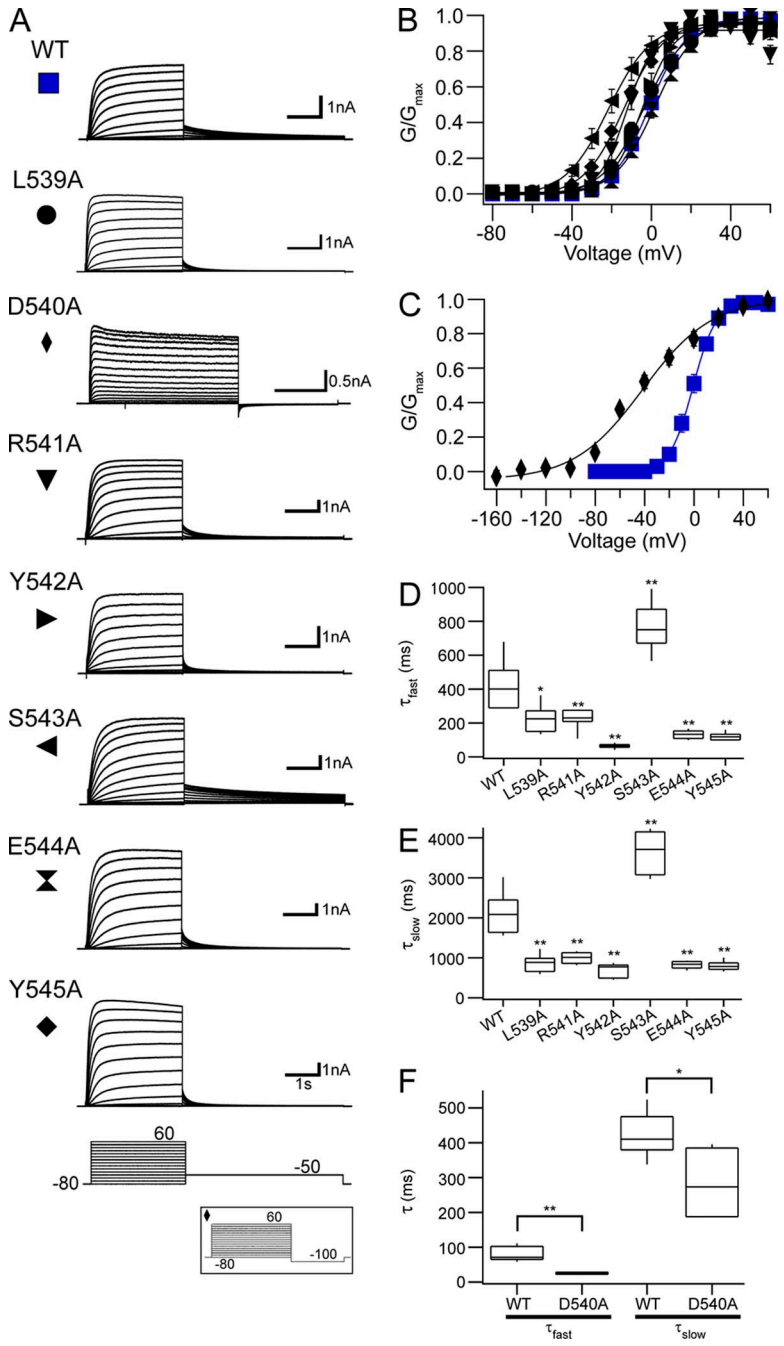

Figure S1. hERG [S4–S5]Ala$_{ind}$ mutant channels exhibit altered gating properties. (A) Representative current recordings from HEK293 cells expressing WT hERG or each hERG [S4–S5]Ala$_{ind}$ mutant channel. The voltage command protocol used to record the ionic currents is shown on the bottom. The inset represents the voltage command protocol used to record hERG D540A currents. (B and C) Voltage dependence of activation (G-V) curves. The tail current amplitudes during the −50-mV pulse were normalized to the maximum tail current amplitude and plotted versus voltage. Plotted points were fit with a Boltzmann function to yield the $V_{1/2}$ and k values (averaged data are given in Table SI). $n \geq 5$ for each. (B) The G-V relationships for WT hERG and each hERG [S4–S5]Ala$_{ind}$ mutant channel, except for hERG D540A. (C) The G-V relationships for WT hERG and hERG D540A. (D and E) Box plots of the time constants of deactivation at −50 mV. Tail currents produced during the −50-mV pulse from 60 mV were fit with a double-exponential function to yield the τ_{fast} (D) and τ_{slow} (E) values. The middle line is the mean, the top and bottom lines are the 75th and 25th percentile, respectively, and the straight lines are the 90th and 10th percentiles. (F) Box plot of the time constants of deactivation at −100 mV. Tail currents produced during the −100-mV pulse from 60 mV were fit with a double-exponential function to yield the τ_{fast} and τ_{slow} values. $n \geq 4$ for each. All data are presented as mean ± SEM. *, $P < 0.05$; **, $P < 0.01$ versus WT hERG (ANOVA).

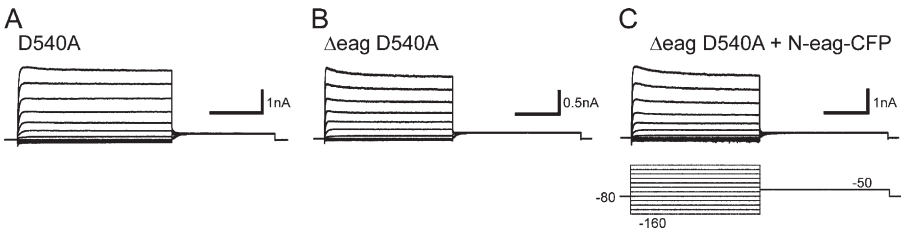

Figure S2. hERG D540A, hERG Δeag D540A, and hERG Δeag D540A + N-eag-CFP currents. Representative ionic currents from HEK293 cells expressing (A) hERG D540A, (B) hERG Δeag D540A, and (C) hERG Δeag D540A + N-eag-CFP using the voltage command protocol shown. From a holding potential of −80 mV, cells were stepped to a series of potentials ranging from −160 to 60 mV in 20-mV increments, followed by a pulse to −50 mV. The peak current amplitudes during each −50-mV pulse were normalized to the maximum current amplitude during the −50-mV pulse and plotted versus voltage. The plotted points were fit with a Boltzmann function to yield the steady-state voltage dependence of activation curve (shown in Figs. S1 C and 2 D).

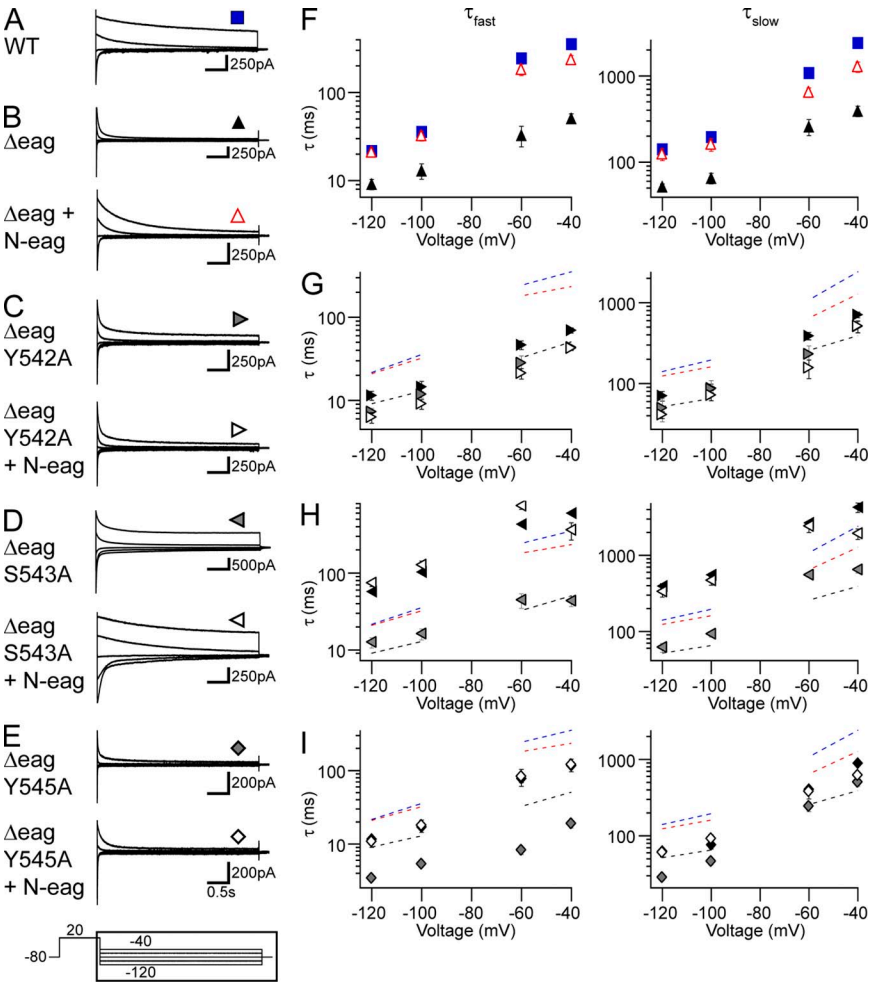

Figure S3. Eag domain regulation of deactivation in the hERG [S4–S5]Ala_{ind} mutant channels. A family of tail currents recorded from HEK293 cells expressing (A) WT hERG, (B) hERG Δeag with or without N-eag-CFP, (C) hERG Δeag Y542A with or without N-eag-CFP, (D) hERG Δeag S543A with or without N-eag-CFP, and (E) hERG Δeag Y545A with or without N-eag-CFP. The pulse protocol used to elicit the tail currents is shown at the bottom; the rectangle represents the region of the current that was expanded and shown in A–E. (F–I) Tail currents were fit with a double-exponential function to yield τ_{fast} and τ_{slow} values. The averaged τ_{fast} (left plots) and τ_{slow} (right plots) are plotted in F–I on a logarithmic scale, which correspond with A–E, respectively, and are also given in Table S2. In G–I, dashed lines represent the τ_{fast} and τ_{slow} values for WT hERG (blue), hERG Δeag (black), or hERG Δeag + N-eag-CFP (red). Black symbols represent the τ_{fast} and τ_{slow} values for the full-length hERG [S4–S5]Ala_{ind} mutant channel. $n \geq 3$ for each. All data are presented as mean ± SEM.